Two-dimensional modeling of the back amorphous-crystalline silicon heterojunction (BACH) photovoltaic device

Zahidur R. Chowdhury[a], Alongkarn Chutinan[a], Adel B. Gougam[b], Nazir P. Kherani[*a,c], and Stefan Zukotynski[a]

[a]Department of Electrical and Computer Engineering, University of Toronto, 10 King's College Road, Toronto, Ontario, Canada M5S 3G4;
[b]Arise Technologies Corp. 65 Northland Road, Waterloo, Ontario, Canada N2V 1Y8;
[c]Department of Material Science and Engineering, University of Toronto, 184 College Street, Toronto, Ontario, Canada M5S 3E4.

ABSTRACT

Back Amorphous-Crystalline Silicon Heterojunction (BACH)[1] solar cell can be fabricated using low temperature processes while integrating high efficiency features of heterojunction silicon solar cells and back-contact homojunction solar cells. This article presents a two-dimensional modeling study of the BACH cell concept. A parametric study of the BACH cell has been carried out using Sentaurus after benchmarking the software. A detailed model describing the optical generation is defined. Solar cell efficiency of 24.4% is obtained for AM 1.5 global spectrum with V_{OC} of greater than 720 mV and J_{SC} exceeding 40 mA/cm^2, considering realistic surface passivation quality and other dominant recombination processes.

Keywords: Solar cell, back-contact, heterojunction, BACH, simulation, Sentaurus

1. INTRODUCTION

High-efficiency crystalline silicon solar cells are predominantly fabricated using high temperature processes. These processes can result in significant thermal stresses in silicon wafers, adversely affect the semiconductor properties of the absorber, and further exacerbate fabrication of cells using thinner wafers. Alternatively, the recently proposed Back Amorphous-Crystalline Silicon Heterojunction (BACH) solar cell can be fabricated using low temperature processes while integrating high efficiency features of heterojunction silicon solar cells and back-contact homojunction solar cells.

The objective of the low-temperature processed BACH cell is to avoid shadowing losses by relegating electrical contacts to the back surface, to minimize ohmic losses by maximizing the width of the alternating metal contacts, to minimize surface recombination of carriers through optimum surface passivation and/or configuration of the contacts, and to implement favorable light trapping features in order to attain the highest conversion efficiency possible.

Back-contact back-junction cell by SunPower also uses contacts at the back for homojunction cells and it has been demonstrated that it is possible to reach a cell efficiency of 24.2% for mass production.[2,3] Lu *et. al.* used Sentaurus[4] to simulate a cell with a similar configuration as the BACH cell; the cell is referred as Interdigitated Back-Contact Silicon HeteroJuction (IBC-SHJ) cell. The authors reported a maximum cell efficiency of 22% for IBC-SHJ considering 300 μm thick crystalline silicon (c-Si) absorber. Aluminium was considered as a contact metal for both electrodes. The width of the doped regions at the back were varied to obtain the maximum efficiency while maintaining the width of a unit cell constant. An AM1.5G solar spectrum was used for optical generation; but a description of the model used for optical generation was not provided.

This article presents a two-dimensional modeling study of the BACH cell concept. A parametric study of the BACH cell has been carried out using Sentaurus. Detailed description of the model used for optical generation is given in this article. A reference case is used in the article to benchmark Sentaurus before using the software for BACH cell simulation. Finally, a range of cell parameters are scanned, including substrate thickness, pitch and passivation quality for cell design optimization.

* E-mail: kherani@ecf.utoronto.ca

Photonics North 2010, edited by Henry P. Schriemer, Rafael N. Kleiman, Proc. of SPIE Vol. 7750, 77502V · © 2010 SPIE · CCC code: 0277-786X/10/$18 · doi: 10.1117/12.872942

2. DEVICE STRUCTURE

A schematic diagram of the simplified BACH cell structure is shown in Figure 1. N-type crystalline silicon wafers with $1\Omega - cm$ resistivity and of different thicknesses are considered as absorber layers. Front surface is considered to be textured with a Lambertian surface, where an incident light is scattered randomly in all directions with equal probability. Moreover, the substrate is passivated with 70 nm thick Si_3N_4 layer at both front and back surfaces. On the rear-side of the wafer, there are 10 nm thick interdigitated strips of p and n amorphous silicon (a-Si) layers. Ideal ohmic contacts on p and n regions are considered for most of the studies, unless otherwise specified. A 100 μm wide n-type a-Si region that functions as a back surface field (BSF) and $100\mu m$ gap between n and p regions are considered. 100 μm features can be easily achieved using photolithographic processes. A narrow BSF field is selected to reduce the effect of electrical shading.[5] The unit cell is considered periodic in the lateral direction with a period defined by the pitch of the cell for the simulations.

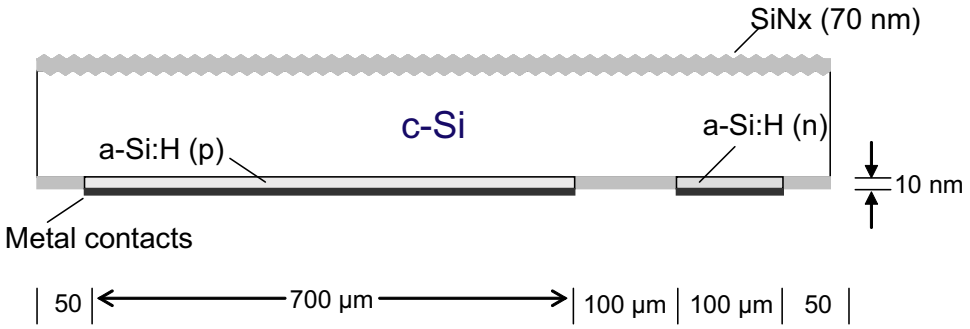

Figure 1. Schematic diagram of the BACH cell.

3. PHYSICAL MODELS

Sentaurus is used to simulate the physics of BACH cell by solving Poisson's equation and Electron/Hole Continuity equations along with Drift-Diffusion electron transport relationship. A thermionic emission model is considered for the heterojunction interface. Independent Auger Shockley-Read-Hall recombination are included or excluded for different cases. Exponential Band-tail and Gaussian band-gap defect distributions of the a-Si layers are chosen.[6]

4. BENCHMARKING SENTAURUS

Sentaurus is a commercially available semiconductor device simulation software that is widely used for electronic structures. Even though Sentaurus is recently being used for solar cell simulation,[7–11] there has been no report that describes how optical absorption in the material is represented in Sentaurus. In this article optical absorption by Beer-Lambert's law is utilized. Moreover, optical intensity distributions for different wavelength or photon energy at the front and back surfaces are calculated to give the carrier generation considering Lambertian front surface and perfectly reflective back surface. Tiedje *et. al.*[12] has considered such surface conditions for c-Si substrate and analytically estimated the theoretical limit of photovoltaic cell efficiencies for different silicon thicknesses. Results obtained in that study are reproduced using Sentaurus for the purpose of benchmarking the software for this application.

In the reference work reported by Tiedje *et. al.*,[12] only a crystalline silicon absorber layer with no pn-junction is considered. No carrier transport mechanism was considered and generated electrons and holes were assumed to be collected where they were generated. Moreover, the optical absorption was also considered to be uniform over the entire c-Si substrate. Random scattering at the front surface and reflection at the back surface result in multiple reflections of low absorbing light before the rays strike the front surface within an escape cone (Figure

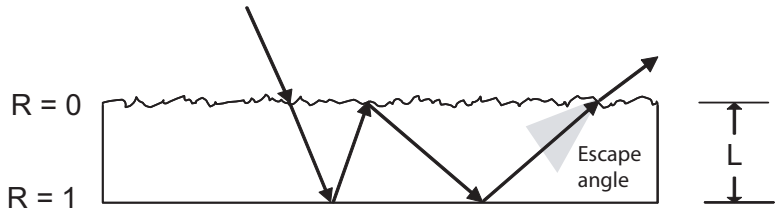

Figure 2. Multiple reflection due to Lambertian front surface and perfectly reflective back surface. Light escapes when it strikes the front surface within an escape cone.

2). Therefore, light absorption is enhanced and the absorption probability for this condition can be expressed by Equation 1,

$$a(E) = \frac{\alpha(E)}{\alpha(E) + \frac{1}{4n(E)^2 L}} \tag{1}$$

where a is the absorption probability, α is the absorption coefficient for a particular photon energy (E), n is the refractive index, and L is the thickness of the absorbing layer. In the case of a low absorption coefficient, for example, in the near infrared, the absorption is enhanced by almost 40 times. This absorption process is different from the case of an untextured surface in which case light absorption follows the Beer-Lamberts law shown in Equation 2:

$$a(E) = 1 - \exp\left[-\alpha(E)L\right] \tag{2}$$

In contrast to Tiedje's model, a highly-doped p-n junction can be defined in Sentaurus to accurately model the carrier transport and collection. A physical optical absorption model can be used where optical generation is larger near the front surface due to front illumination.

4.1 Optical Generation

The most accurate method to represent optical generation is probably by solving Maxwell's equation. The second method, used by many solar cell simulation softwares is to calculate the field distribution using the Transfer Matrix method. This method considers multiple reflections in the longitudinal direction but does not consider the scattering in the lateral directions. This method is supported by Sentaurus but there is an issue with the accuracy of the transfer matrix module in Sentaurus. As a consequence, Beer-Lambert's model, which is supported in Sentaurus, is used to represent optical generation in the absorbing layer. This model considers a simple exponential decay and it does not consider any multiple reflection or lateral scattering.

Optical intensity distributions, incident at the front surface and reflected at the back surface, are modified to consider absorption due to multiple reflections. An effective length to represent the same absorption due to scattering and multiple reflections by Beer-Lambert's law is calculated first. Subsequently the number of reflections is considered based on the length of the substrate and the effective length. The initial intensity at a reflective surface is scaled when the light has to travel a fraction of the substrate thickness to represent the same absorption. The light intensity for different photon energies at the front and back surfaces are expressed by Equation 3 and 4.

$$S_f(E) = \sum_{m=0}^{M(E)} S_{fm}(E) = \sum_{m=0(\text{even})}^{M(E)} s_m(E) S_0(E) \exp\left[-m\alpha(E)L\right] \tag{3}$$

$$S_b(E) = \sum_{n=0}^{N(E)} S_{bn}(E) = \sum_{n=1(\text{odd})}^{N(E)} s_n(E) S_0(E) \exp\left[-n\alpha(E)L\right] \tag{4}$$

In the above equations, S_f and S_b are the total intensity for a particular photon energy at the front and back surfaces, respectively. M and N are the indexes representing the total number of reflections at the front and back surfaces, respectively. S_{fi} (*i.e.* S_{fm} or S_{fn}) is the intensity at the surface for the i-th reflection, s_i is

the scaling factor of i-th reflection and S_0 is the peak intensity for a photon energy defined by AM1.5G solar spectrum.

Since S_f and S_b are calculated based on thickness dependent absorption (Equation 1), these parameters are also thickness dependent and a separate numerical software, other than Sentaurus, is used to calculate these values for different thicknesses.

5. RESULT AND DISCUSSION

5.1 Benchmarking Results

As mentioned earlier that in the reference article no pn-junction was considered for carrier transport while a device structure has to be considered with appropriate transport mechanisms for the numerical simulation. Moreover, according to the expressions derived in that article the characteristics of the cell depends on dark current, optical generation and recombination parameters. Dark current was calculated from black-body radiation in that article and was a very small value (1.7×10^{-13} mA/cm^2). Therefore, any photovoltaic cell structure can be used to reproduce the results of reference article as long as the same parameters are used. BACH cell structure is preferred since it is going to be used eventually.

Figure 3 shows comparison of theoretical results of the reference case and the results obtained for BACH cells when identical parameters for c-Si substrates are considered. Short-circuit current, J_{SC}, is observed to increase with increasing substrate thickness while the V_{OC} decreases. Auger recombination is the more dominant recombination mechanism for high carrier concentrations and this recombination process significantly reduces the open-circuit voltages, V_{OC}.

No surface recombination or SRH recombination is considered in this case. Moreover, for all simulation results for the BACH cell the absorption in the passivation layer and resistive loss at the metal contacts are ignored. As shown in the figure, there is a close match between theoretical results of the reference case and the numerical simulation results by Sentaurus.

5.2 BACH Simulation Results

The optical spectrum considered in the reference case was that recommended by SERI.[13] Total intensity of the spectrum was 97 mW/cm^2. Currently the total intensity standard recommended by ASTM is 100 mW/cm^2. Moreover, the Auger recombination coefficient is higher compared to the one considered by the reference case for high carrier injection in solar cells.[14] The short-circuit currents and open-circuit voltages for different thicknesses are plotted in Figure 4 for two different spectral standards and recombination coefficients. The short-circuit-currents for different thicknesses are higher for the ASTM spectrum. The open-circuit-voltages are lower for

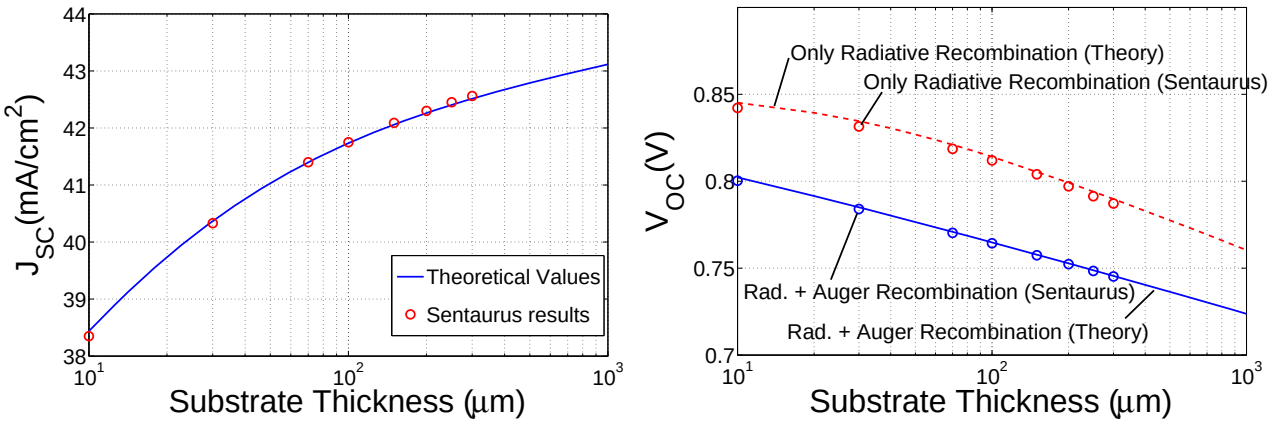

Figure 3. Comparison of short-circuit-currents(left) and open-circuit-voltages(right) for different considerations of reference case and Sentaurus simulation results.

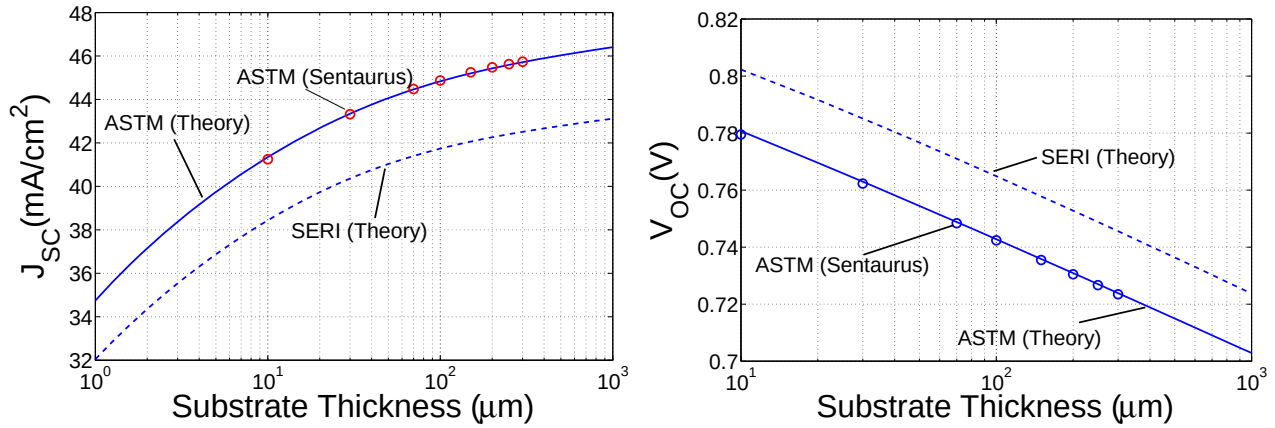

Figure 4. Effect of using current solar spectrum standard (ASTM) and Auger recombination coefficients for high carrier injection

this case due to higher carrier concentration and higher Auger recombination coefficient. A close match between analytically calculated (theoretical) and numerically simulated values is observed for both J_{SC} and V_{OC}.

Defects at interfaces have a strong influence on effective carrier lifetime as well as cell performance. Surface recombination velocity (SRV) represents passivation quality, *i.e.*, a representation of the density of interface/surface defects. Figure 5 shows the effect of surface passivation in cell performance. The cell performance deteriorates with poorer passivation (higher SRV values). The performance or efficiency of cells thinner than 50 μm and thicker than 150 μm is more severely affected by higher SRV values.

Carrier concentration is higher at the front surface due to front illumination. For very thin substrates these excess carriers recombine at the front surface and also in the gap regions between the doped areas of the back surfaces due to SRV. On the other hand, when substrates are very thick, carriers recombines at the front surface and in the bulk before being collected by the two electrodes as well as in the gap regions. For an SRV of 10 cm/s, the maximum efficiency was observed for substrate thickness of 100 μm. Surface passivation giving an SRV of 10 cm/sec can be achieved by thermal oxide passivation layers[15] and thin thermal oxide and PECVD grown nitride layers.[16]

Cell design is also optimized by varying the pitch of the cell. Minimum gap and minimum width of the BSF region of 100 μm are considered on the back-side to reduce rear surface recombination and electrical shading loss, respectively. Hence, varying the pitch in effect is varying the width of the emitter (p-doped region) while

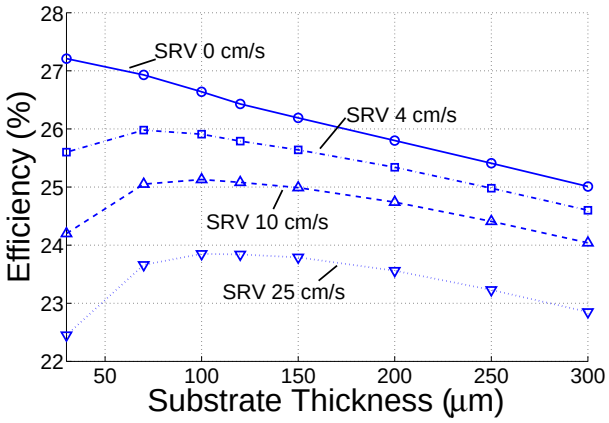

Figure 5. Cell performance for different surface passivation quality (SRV).

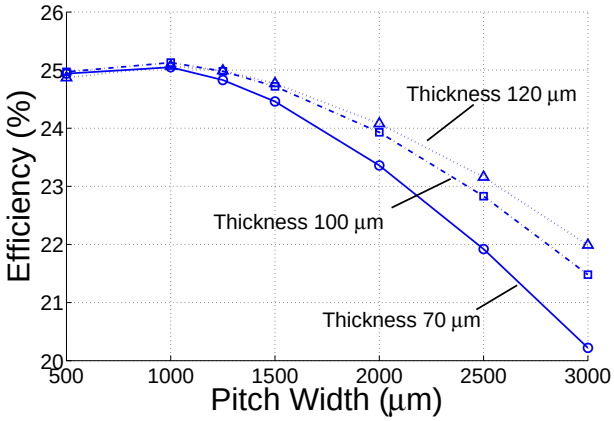

Figure 6. Cell performance for different width of unit cell or pitch size.

maintaining other feature sizes constant. Figure 6 shows the effect of pitch variation for different thickness. The optimum value of the pitch is 1 mm. The electrical shading loss becomes dominant for smaller pitch size since BSF width becomes comparable to the emitter width.

Finally, work-function of the metal electrodes is introduced to provide a more representative BACH cell simulation. Nickel is used as the anode and aluminum is used as the cathode representing contacts close to being perfectly ohmic. Figure 7 shows the variation of efficiency for different cell thicknesses with 1 mm pitch. An SRV of 10 cm/sec and other recombination processes are also considered. As mentioned earlier, no absorption is considered in the SiNx passivation layers. It should also be noted that the resistive loss at the metal contacts depends on the grid pattern and metal thickness. Such loss was also not considered in the current simulations. The maximum efficiency is 24.4% with $J_{SC} = 43.87\ mA/cm^2$, $FF = 77.04\%$ and $V_{OC} = 0.722\ V$.

6. CONCLUSION

BACH cell simulation results are presented in this article considering a Lambertian front surface and reflective back surface. Optical intensity is calculated at the two surfaces to ensure proper optical generation using Beer-Lambert's law for optical absorption. Cell performances for different absorber layer thicknesses, passivation parameters, electrode spacings are considered. The maximum efficiency is 24.4% for the simulated cell structure

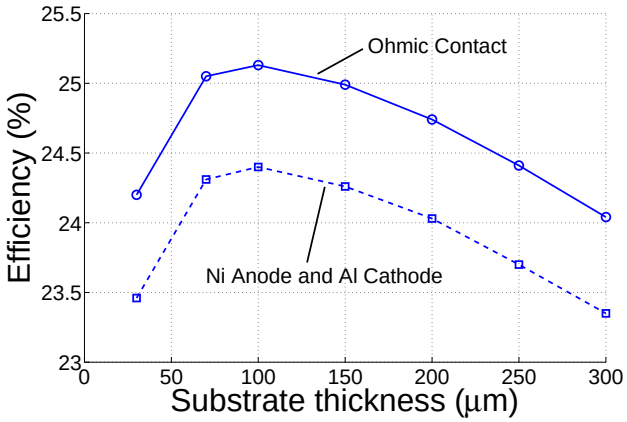

Figure 7. Effect of metal work-function. Nickel anode and Aluminum cathode give a maximum efficiency of 24.4% for other optimized condition.

for 100 μm thick c-Si absorbing layer with passivation layers having 10 cm/sec SRV. Radiative, Auger and SRH recombination are also considered. The optimum cell configuration has 100 μm wide gap between emitter and BSF. The width of the BSF and emitter is 100 μm and 700 μm, respectively. Resistive loss in the metal and absorption loss in the passivation layers were not considered in this series of simulation.

ACKNOWLEDGMENTS

The work was supported through grants from Natural Sciences and Engineering Research Council of Canada, Ontario Centers of Excellence, and the Ontario Research Fund Research Excellence program, in collaboration with Arise Technologies Corporation.

ZRC would like to express his gratitude to Dr. Honggang Liu for the introduction to Sentaurus.

REFERENCES

[1] Hertanto, A., Liu, H., Yeghikyan, D., Rayaprol, B. G., Kherani, N. P., and Zukotynski, S., "Back amorphous-crystalline silicon heterojunction (BACH) photovoltaic device," *IEEE 34th PVSC* (2009).

[2] Ceuster, D. M. D., Cousins, P., Rose, D., Vicente, D., Tipones, P., and Mulligan, W., "Low cost, high volume production of >22% efficiency silicon solar cells," *Proceedings of the 22nd European Photovoltaic Solar Energy Conference* .

[3] Release, S. P., "Sunpower announces new world record solar cell efficiency - full-scale prototype produced at 24.2 percent," (23 June, 2010). http://investors.sunpowercorp.com/releases.cfm.

[4] Synopsys, "Vol.Release A-2008.09," (2008). http://www.synopsys.com.

[5] Dross, F., VanKerschaver, E., and Beaucarne, G., "Minimization of the shadow-like losses for inter-digitated back-junction solar cells," *Proceedings of the 15th International Photovoltaic Science and Engineering Conference* .

[6] Schropp, R. E. I. and Zeeman, M., [*Amorphous and micro-crystalline silicon solar cells*], Kluwer Academic, Dordrecht, Netherland (1998).

[7] Nichiporuk, O., Kaminski, A., Lemiti, M., Fave, A., and Skryshevsky, V., "Optimisation of interdigitated back contacts solar cells by two-dimensional numerical simulation," *Solar Energy Materials and Solar Cells* **86(4)**, 517–526 (2005).

[8] Hermle, M., "Analyse neuartiger silizium und iiiv-solarzellen mittels simulation und experiment," *Universität Konstanz, Dissertation thesis* (2008).

[9] Lu, M., Bowden, S., and Birkmire, R., "Two dimensional modeling of interdigitated back contact silicon heterojunction solar cells," *Conference on Numerical Simulation of Optical Device* , 55–56 (2007).

[10] Lu, M., "Silicon heterojunction solar cell and crystallization of amorphous silicon," *University of Delaware, , Dissertation thesis* (2008).

[11] Renshaw, J., Kang, M., Meemongkolkiat, V., Rohatgi, A., Carlson, D., and Bennett, M., "3D-modelling of a back point contact solar cell structure with a selective emitter," *Conference Proceedings of the 34th IEEEPVSC* (2009).

[12] Tiedje, T., Yablonovitch, E., Cody, G. D., and Brooks, B. G., "Limiting efficiency of silicon solar cells," *IEEE Transaction on Electron Devices* **31(5)**, 711–716 (1984).

[13] Matson, R., Bird, R., and Emery, K., "Terrestrial solar spectra, solar simulation and solar cell short-circuit current calibration: A review," *Solar Cells* **11**, 105–145 (1984).

[14] Sinton, R. A. and Swanson, R. M., "Recombination in highly injected silicon," *IEEE Transactions of Electron Device* **34(6)**, 1380–1389 (1987).

[15] Hoex, B., Schmidt, J., Pohl, P., van de Sanden, M. C. M., and Kessels, W. M. M., "Silicon surface passivation by atomic layer deposited Al_2O_3," *Journal of Applied Physics* **104**, 044903 (2008).

[16] Larionova, Y., Mertens, V., Harder, N.-P., and Brendel, R., "Surface passivation of n-type Czochralski silicon substrates by thermal-SiO_2/plasma-enhanced chemical vapor deposition SiN stacks," *Applied Physics Letters* **96**, 032105 (2010).